High-resolution spin-flip Raman scattering in CdTe quantum wells at ^{3}He temperature

R. Shen,[1] K. Oto,[2] K. Muro,[2] G. Karczewski,[3] T. Wojtowicz,[3] J. Kossut,[3] and S. Takeyama[1]
[1]*Institute for Solid State Physics, University of Tokyo, 277-8581 Kashiwa, Japan*
[2]*Department of Physics, Chiba University, 263-8522 Chiba, Japan*
[3]*Institute of Physics, Polish Academy of Sciences, 02-668 Warsaw, Poland*
(Received 7 May 2009; revised manuscript received 13 July 2009; published 15 September 2009)

The high-resolution spin-flip Raman-scattering experiments were carried out on high-quality CdTe quantum wells below 0.5 K in high magnetic fields up to 14 T. An obvious exciton spin-flip Raman-scattering signal was observed in each quantum well under the Voigt configuration. The exciton exchange splitting in each quantum well was precisely determined.

DOI: 10.1103/PhysRevB.80.125312 PACS number(s): 78.30.Fs, 71.35.Ji, 71.70.Gm, 78.67.De

I. INTRODUCTION

The (short-range) electron-hole exchange interaction results in splitting of the fourfold-degenerate exciton (heavy-hole exciton) levels into one optical allowed ($J=1$) doublet and another forbidden ($J=2$) doublet.[1] This interaction sensitively depends on the spatial extension of the electron-hole wave-function overlap and is predicted to enhance with increasing the dimensional confinement.[2,3] Good experimental approach has been first performed in type-II GaAs/AlAs quantum wells (QWs) by optically detected magnetic resonance, when applied to the restricted excitonic system having a long lifetime ($>\mu$s).[4] On the other hand, there has been a well-defined report investigating the exciton energy splitting in type-I GaAs QW (the exciton lifetime $\ll\mu$s) by analyzing peculiarities of the exciton photoluminescence (PL) circular polarizations arising from the level crossing (or anticrossing) of the excitonic states in magnetic fields.[5] These approaches in the QWs are much more efficient than those in the quantum wires or quantum dots (QDs) for presenting obviously the contribution of the confinement effects on the exchange interaction since only one dimension is reduced. Recently, there has been an exemplary study in (Zn,Cd)Se multiple QWs investigated by the spin-flip Raman scattering (SFRS),[6] which performed a direct observation of the spin relaxation between the split excitonic states, also not restricted by the exciton lifetime. However, the result of this study is very similar to that obtained in nanocrystals (i.e., QDs) (Refs. 7 and 8) because of strong localization of the excitons caused by the alloy disorders. To our best knowledge, there is still no report about fine structures of the free exciton in an ideal two-dimensional system performed by this direct observation of the spin relaxation since the splitting energy is considered to be much smaller than the results of the earlier studies. Therefore, in order to fully clarify the spin splitting of the free exciton in a QW, a highly-sensitive and high-resolution experiment is strongly desired. Furthermore, the measurement is desirable for being performed at ultralow temperatures because it is well known that the thermal activation may cause mixing of the spin states.

We have therefore developed a homemade resonant SFRS spectroscopy system at a ^{3}He temperature in magnetic fields up to 14 T by utilizing optical fibers.[9] In this paper, we present results of an exciton-spin-flip Raman-scattering (XSF) as well as an electron-spin-flip Raman-scattering (ESF) signal in CdTe QWs performed at such low temperatures. This XSF signal became more obvious with increasing the exciton density induced by a pump laser. As a result, the spin-splitting energy of the free exciton ground state, which is also determined as the electron-hole exchange interaction, was precisely determined in each of our QWs.

II. EXPERIMENTS

We have investigated three different CdTe QWs, which were grown on (001)-oriented substrates by molecular-beam epitaxy. One is a nonmagnetic sample, consisting of a 3.9 nm CdTe well layer sandwiched by a 50 nm nonmagnetic $Cd_{0.85}Mg_{0.15}Te$ barrier on both sides. The other two QWs are dilute magnetic samples, consisting of a CdTe well layer with widths of 3.6 and 4.9 nm sandwiched by a 50 nm dilute magnetic $Cd_{0.8}Mn_{0.2}Te$ barrier on one side and a 50 nm nonmagnetic $Cd_{0.9}Mg_{0.1}Te$ barrier on the other side. The PL and photoluminescence excitation (PLE) spectra of each QW are shown in Fig. 1. The PL spectra show the distinct double-peak structure in each QW. The higher energy line denoted by X in Fig. 1 is attributed to the lowest heavy-hole (*hh*) exciton state. A slight Stokes shift of about 1.0 meV from the peak of the PLE signifies that the *hh* exciton is slightly influenced by localizations due to the alloy or interface disorders in the QW.

The SFRS measurements were performed under the Voigt configuration using a homemade sample holder, which was inserted into a liquid ^{3}He cryostat equipped with a 14 T superconducting magnet. Excitation light from an etalon-tuned Ti:sapphire ring laser (linewidth <0.001 nm) was coupled into the polarization maintaining fiber and was introduced into the ^{3}He cryostat. Luminescence and scattered light were collected by a pair of miniature lenses into the bundle fibers and were introduced to a 1.26 m single-grating spectrometer equipped with a multichannel and liquid nitrogen-cooled charged-coupled device detector. The spectral resolution is 0.02 nm (about 50 μeV in the investigated range). The details of the sample holder and experiments have been described in our previous report.[9] In addition, the circularly polarized PL spectra were measured in a cryostat having optical windows at 1.4 K up to 7 T under the Faraday configuration.

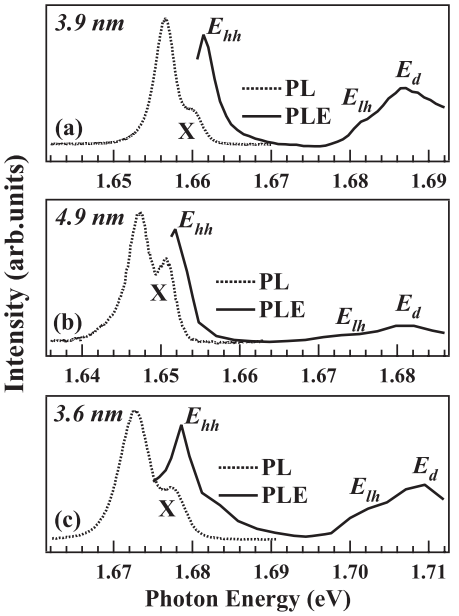

FIG. 1. The PL and PLE spectra of (a) 3.9 nm, (b) 4.9 nm, and (c) 3.6 nm CdTe QWs at 1.4 K, respectively. The X represents the peak of heavy-hole exciton PL spectra. The E_{hh}, E_{lh}, and E_d indicate energy positions of the heavy-hole, the light-hole exciton, and the band edge of the first intersubband transition, respectively.

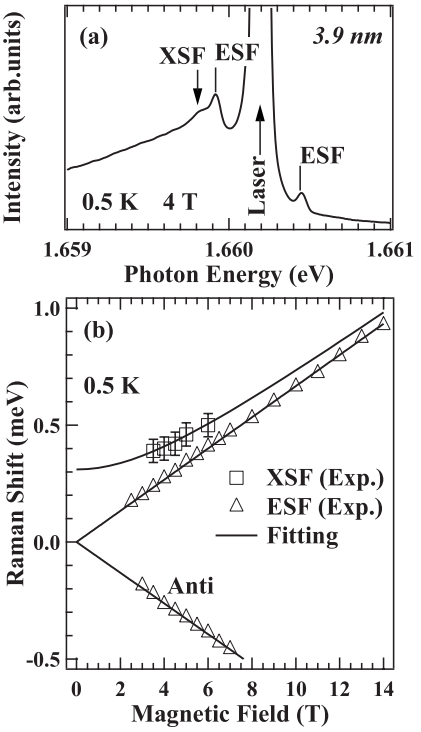

FIG. 2. (a) The SFRS spectra of the 3.9 nm CdTe QW at 0.5 K and 4 T in the Voigt configuration. The photoexcitation density is 1 W/cm^2. (b) Raman shifts of the XSF and ESF spectra in magnetic fields. Lines represent the fit of the experimental data. The Anti indicates an anti-Stokes ESF peak.

III. RESULTS AND DISCUSSIONS

Figure 2(a) shows the SFRS spectra of the 3.9 nm CdTe QW, measured at 4 T and 0.5 K. The photoexcitation energy was set at 1.6602 eV, adjusted to the *hh* exciton resonance. Two sharp Raman lines (the linewidth is about 100 μeV) appear symmetrically placed at the Stokes (a low-energy shift) and anti-Stokes sides. These two lines arise from signals of ESF. A peak structure is observed to lie at a lower energy side of the Stokes ESF line by about 0.2 meV. It is also evident that the linewidth of the Raman peak is broader than those of the ESF. The linewidth broadness and the energy position with respect to the ESF peak resemble well the features of the XSF observed in a ZnSe/(Zn,Cd)Se QW.[6] The energy shifts of three Raman peaks against a magnetic field up to 14 T are plotted in Fig. 2(b). Both ESF peaks show a good linear dependence on magnetic field. Since the electron g factor has a minus sign in CdTe QWs, Raman shifts of the Stokes and anti-Stokes ESF ($\Delta E_e^{\pm}$) can be described by the formula $\Delta E_e^{\pm} = \mp g_{e,x}\mu_B B_x$, where $g_{e,x}$ is the electron g factor component vertical to the growth direction (noted as the z axis), μ_B is the Bohr magneton, and B_x is the magnetic field vertical to the z axis. Fitting the experimental data, a precise value of $g_{e,x}$ is determined as -1.15, of which value is consistent with those obtained by the other group.[10] Since no optically induced carriers (free electrons) are injected from barriers into the well under resonance excitation, the low-density residual electrons in the well are considered as the origin of ESF signals.

The *hh* exciton is considered as an origin of the observed XSF since the light-hole (*lh*) excitons are located at much higher energy ($\approx$20 meV) in the 3.9 nm QW as shown in Fig. 1(a). Furthermore, the *hh* exhibits no Zeeman splitting in the Voigt configuration since its spin is oriented along the z axis.[11] The Raman shift of the XSF (ΔE_X) can be represented by $\Delta E_X = \sqrt{\Delta_X^2 + (g_{e,x}\mu_B B_x)^2}$,[6] where Δ_X is the zero-field energy splitting between the bright ($J=1$) and the dark ($J=2$) excitons (*hh* exciton) caused by the electron-hole exchange interaction.[3,5,6] Using the obtained value of $g_{e,x}$, we can reproduce well the experimental line with a fitting curve, as seen in Fig. 2(b). The result is obtained at a finite value of ΔE_X as 0.31 ± 0.05 meV at 0 T, from which the Δ_X is determined in the 3.9 nm QW.

Figure 3(a) shows the SFRS spectra of a 4.9 nm CdTe QW with a dilute magnetic barrier in magnetic fields at 1.5 and 6 T and in ^{3}He temperature upon the *hh* exciton resonance excitation. There observed multiple (up to three) sharp Stokes Raman peaks lie in equal-energy intervals. One anti-Stokes signal is also observed. The Raman shifts (ΔE_n) against a magnetic field (represented in Fig. 5 below) are reproduced well by $\Delta E_n = n g_{\mathrm{Mn}} \mu_B B_x$, where $g_{\mathrm{Mn}}(\approx 2)$ is the Mn^{2+} g factor and n is an integer. These features are due to Raman transitions between adjacent Zeeman sublevels of the Mn^{2+} ions, usually observed in magnetic CdMnTe QWs.[12–15] Since the linewidth of multi-Mn^{2+} Raman peaks shown in Fig. 3(a) is determined by the spectral resolution of the spectrometer, the observed linewidth is considered as less than 100 μeV in our measurements. Another broader single peak is observed to appear distinctly, whose linewidth is about 200 μeV, as seen in Fig. 3(a). The origin of this broader Raman peak in the 4.9 nm QW is considered the XSF since the ESF linewidth should be sharper.

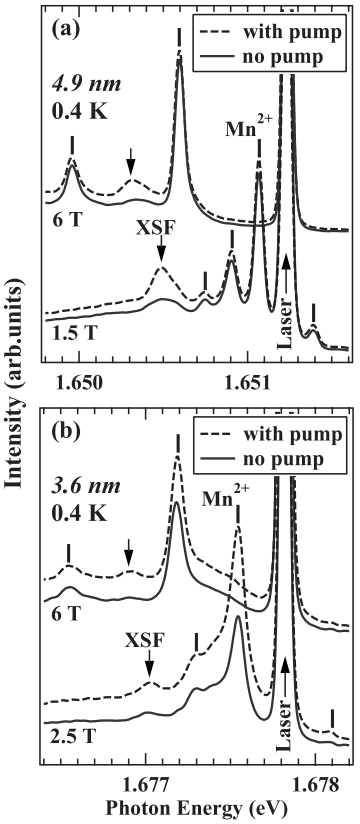

FIG. 3. The solid lines represent SFRS spectra of (a) 4.9 nm and (b) 3.6 nm CdTe QWs in magnetic fields (the Voigt configuration) at 0.4 K, respectively. The photoexcitation density is 1 W/cm^2. The dashed lines show SFRS spectra measured under an external pumping with the photoexcitation density 0.1 W/cm^2.

The SFRS spectra measured with an external laser pumping are shown by the dashed lines in Fig. 3(a). The excitation energy of a pump laser is set at the *lh* exciton resonance (about 20 meV higher-energy side). The broader peak intensity is obviously increased by the external pumping, while there is almost no change in the multi-Mn^{2+} Raman intensities. The external optical pumping with energy below the band gap can create only the electron-hole bound state (exciton) in the QW. Therefore, the broader Raman peak is assigned as the XSF as its origin. Likewise, the clear XSF can be observed, not hidden in the strong multi-Mn^{2+} Raman signals, in the dilute magnetic 3.6 nm QW with an external pumping, as seen in Fig. 3(b).

On the other hand, the electron and hole Zeeman splitting present an unusual magnetic field behavior in dilute magnetic semiconductor systems because of the spin-exchange

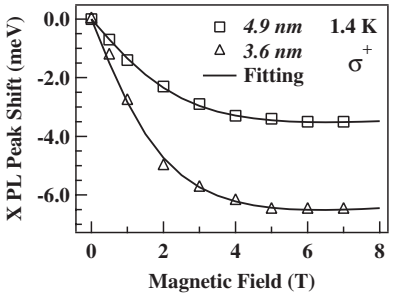

FIG. 4. The peak energy shifts of the exciton (X) σ^+ PL spectra in 4.9 and 3.6 nm CdTe QWs against a magnetic field (the Faraday configuration) at 1.4 K, respectively. Lines represent the fit of the experimental data.

interaction with the magnetic ions.[16,17] Hence, in dilute magnetic 4.9 and 3.6 nm QWs, the electron and *hh* Zeeman splitting ($E_e^{\pm}$ and $E_{hh}^{\pm}$) are modified by

$$E_e^{\pm} = \pm\left(\frac{1}{2}g_e\mu_B B - \frac{1}{2}N_0\alpha x\langle S_B\rangle\right), \quad (1)$$

$$E_{hh}^{\pm} = \mp\left(\frac{1}{2}g_{hh}\mu_B B - \frac{1}{2}N_0\beta x\langle S_B\rangle\right), \quad (2)$$

respectively, where g_e and g_{hh} are the components of electron and *hh* g factors along the direction of a magnetic field in CdTe QWs, respectively, B is the magnetic field, $N_0\alpha(\approx 220$ meV) and $N_0\beta(\approx -880$ meV) are the values determined by the *s-d* and *p-d* exchange interactions, respectively, x is the concentration of Mn^{2+} ions (in the barrier layer), and $\langle S_B\rangle$ is the thermal average value of the Mn^{2+} spin parallel to the magnetic field. Hence, $\langle S_B\rangle = -S_0 B_S[\frac{Sg_{\mathrm{Mn}}\mu_B B}{k_B(T_0+T_{\mathrm{sy}})}]$, where S_0 is the effective Mn^{2+} spin, B_S is the Brillouin function, $S(=\frac{5}{2})$ is the total Mn^{2+} spin, T_0 is the effective temperature of the Mn^{2+} spin system, and T_{sy} is the system temperature.

Figure 4 shows the peak energy shifts of right circularly polarized (σ^+) exciton PL spectra in magnetic fields (in the Faraday configuration) for two QWs with a dilute magnetic barrier at 1.4 K. Both peaks show a strongly nonlinear dependence until saturation at a high magnetic field. To avoid the heating of the Mn^{2+} spin system, the photoexcitation density is kept as low as 0.01 W/cm^2.[18] Hence, T_{sy} can be set to 1.4 K, which is the same as the ambient temperature. The experimental curves in Fig. 4 are well fitted by the formula $E_e^- + E_{hh}^-$ according to Eqs. (1) and (2), where the $g_{e,z}$ and $g_{hh,z}$ (noted as the components along the z axis) of two QWs are taken from Ref. 10, respectively. Then, the values of $x \cdot S_0$

TABLE I. The electron and heavy-hole g factors and parameters of magnetization function in 4.9 and 3.6 nm CdTe QWs, respectively.

QW (nm)	$g_{e,x}$	$g_{e,z}$	$g_{hh,z}$	$x \cdot S_0$	T_0 (K)
4.9	−1.2	−1.4	0.8	0.0083	3.34
3.6	−1.1	−1.3	1.0	0.0217	4.0

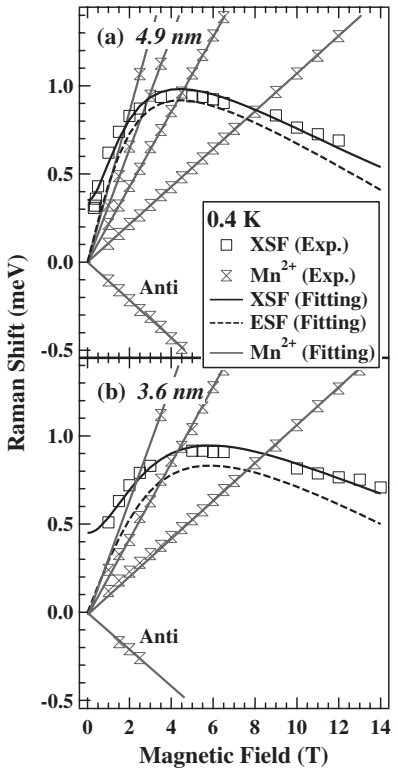

FIG. 5. The peak energy shifts of XSF and multi-Mn^{2+} Raman spectra in magnetic fields, in (a) 4.9 nm and (b) 3.6 nm CdTe QWs, respectively. The solid lines represent the fit of experimental data. The Anti indicates an anti-Stokes Mn^{2+} Raman peak. The dashed lines present the simulation of ESF Raman shifts in two QWs with the formula $|g_{e,x}\mu_B B_x - N_0\alpha x\langle S_B\rangle|$.

and T_0 in two QWs are obtained and listed in Table I.

The peak energy shifts of XSF and multi-Mn^{2+} Raman spectra in 4.9 and 3.6 nm QW against a magnetic field up to 14 T are plotted in Figs. 5(a) and 5(b), respectively. The behavior of each Mn^{2+} Raman peak shows a good linear dependence and is well reproduced by a solid line fitted by $ng_{\mathrm{Mn}}\mu_B B_x$ in both QWs. In contrast, each of the XSF peaks show a Brillouin function like behavior. Modified by Eq. (1), the *Puls*'s formula[6] can be described by $\Delta E_X = \sqrt{\Delta_X^2 + (g_{e,x}\mu_B B_x - N_0\alpha x\langle S_B\rangle)^2}$ in dilute magnetic CdTe QWs. According to the parameters listed in Table I, the fitting curves well reproduce our experimental observations of the XSF in both QWs, where the $g_{e,x}$ of two QWs are approximately gained from Ref. 10. Then, the Δ_X and T_{sy} of each QW are precisely determined and listed in Table II, respectively. Both T_{sy} of two QWs are higher than the ambient temperature (0.4 K), which suggests that the heating of the system is caused by photoexcitation.[18]

TABLE II. The zero-field splitting energies of the heavy-hole exciton and system temperatures obtained from the XSF measurements in 4.9 and 3.6 nm CdTe QWs, respectively.

QW (nm)	Δ_x (meV)	T_{sy} (K)
4.9	0.35 ± 0.02	0.6
3.6	0.45 ± 0.02	1.0

The present result that the Δ_X of the narrow QW is larger than that of the wide one is in accordance with that in GaAs QWs, in which they found that the electron-hole spin exchange increases with the reduction in well widths.[2,5] This fact is more evidence of the XSF for the observed broader Raman peaks in two QWs.

Δ_X about 0.1 meV was reported in a bulk CdTe.[19] Therefore, the enhancement factors of the Δ_X caused by the quantum confinement in our case are 3–5. These results are also similar to those obtained in other II–VI QWs (Ref. 6) as well as in the theoretical expectation.[2]

IV. CONCLUSIONS

We have performed a high-resolution SFRS spectroscopy in CdTe QWs at ^{3}He temperature (below 0.5 K). The exciton spin-flip Raman signal was observed in all investigated QWs. The intensity of the signal grew with the increase in the exciton density induced by a pump excitation. By analyzing Raman shifts of the spectra, the zero-field exchange splitting of the heavy-hole exciton in each QW is precisely determined. Thus our developed method of two-beam SFRS spectroscopy, which can effectively enhance the sensitivity of the excitonic signal, is expected to be a powerful technique for unraveling the fine structure of the excitonic systems.

ACKNOWLEDGMENTS

This work was supported by a Grant-in-Aid for Scientific Research on Priority Areas "High Field Spin Science in 100 T" (No. 451) from the Ministry of Education, Culture, Sports, Science and Technology (MEXT) of Japan.

[1] G. L. Bir and G. E. Pikus, *Symmetry and Strain-Induced Effects in Semiconductors* (Wiley, New York, 1975).
[2] Y. Chen, B. Gil, P. Lefebvre, and H. Mathieu, Phys. Rev. B **37**, 6429 (1988).
[3] M. Z. Maialle, E. A. de Andrada e Silva, and L. J. Sham, Phys. Rev. B **47**, 15776 (1993).
[4] H. W. van Kesteren, E. C. Cosman, W. A. J. A. van der Poel, and C. T. Foxon, Phys. Rev. B **41**, 5283 (1990).
[5] E. Blackwood, M. J. Snelling, R. T. Harley, S. R. Andrews, and C. T. B. Foxon, Phys. Rev. B **50**, 14246 (1994).
[6] J. Puls, F. Henneberger, M. Rabe, and A. Siarkos, J. Cryst. Growth **184-185**, 787 (1998).
[7] T. Ruf, O. Z. Karimov, D. Wolverson, J. J. Davies, A. N. Reznitsky, A. A. Klochikhin, S. Yu. Verbin, L. N. Tenishev, S. A. Permogorov, and S. V. Ivanov, Physica B **273-274**, 911 (1999).
[8] O. Z. Karimov, D. Wolverson, J. J. Davies, T. Ruf, and L. N. Tenishev, Phys. Status Solidi B **215**, 373 (1999).

[9] K. Arahara, T. Koyama, K. Oto, K. Muro, S. Takeyama, G. Karczewski, T. Wojtowicz, and J. Kossut, J. Phys.: Conf. Ser. **51**, 533 (2006).
[10] A. A. Sirenko, T. Ruf, M. Cardona, D. R. Yakovlev, W. Ossau, A. Waag, and G. Landwehr, Phys. Rev. B **56**, 2114 (1997).
[11] R. W. Martin, R. J. Nicholas, G. J. Rees, S. K. Haywood, N. J. Mason, and P. J. Walker, Phys. Rev. B **42**, 9237 (1990).
[12] J. Stühler, G. Schaack, M. Dahl, A. Waag, G. Landwehr, K. V. Kavokin, and I. A. Merkulov, Phys. Rev. Lett. **74**, 2567 (1995).
[13] M. Byszewski, D. Plantier, M. L. Sadowski, M. Potemski, A. Sachrajda, Z. Wilamowski, and G. Karczewski, Physica E (Amsterdam) **22**, 652 (2004).
[14] J. M. Bao, A. V. Bragas, J. K. Furdyna, and R. Merlin, Phys. Rev. B **71**, 045314 (2005).
[15] L. C. Smith, J. J. Davies, D. Wolverson, M. Lentze, J. Geurts, T. Wojtowicz, and G. Karczewski, Phys. Rev. B **77**, 115341 (2008).
[16] J. A. Gaj, R. Planel, and G. Fishman, Solid State Commun. **29**, 435 (1979).
[17] J. K. Furdyna and J. Kossut, *Semiconductors and Semimetals*, Diluted Magnetic Semiconductors Vol. 25 (Academic, San Diego, 1988).
[18] D. Keller, D. R. Yakovlev, B. König, W. Ossau, Th. Gruber, A. Waag, L. W. Molenkamp, and A. V. Scherbakov, Phys. Rev. B **65**, 035313 (2001).
[19] W. Dreybrodt, K. Cho, S. Suga, F. Willmann, and Y. Niji, Phys. Rev. B **21**, 4692 (1980).